CHINESE JOURNAL OF PHYSICS VOL. 36, NO. 4 AUGUST 1998

Coherent Transient Optical Kerr Effect in Liquids: Experimental Consideration

Tzer-Hsiang Huang[1,†], Chia-Chen Hsu[1], Tai-Huei Wei[1], Michael Jiunn Chen[1], Chao-Ming Fu[2], and Ju-Iang Chen[2]

[1] *Department of Physics, National Chung-Cheng University, Ming-Hsiung, Chia-Yi, Taiwan 621, R. O. C.*

[2] *Department of Physics, National Kaoshiung Normal University, Kashiung, Taiwan 802, R. O. C.*

(Received April 10, 1998)

The noise tenaciously appearing in the optically heterodyne detected (OHD) transient optical Kerr effect (OKE) of simple molecular liquids is investigated. We show that, for liquid samples of interest to us, coherent coupling does exist and appears as noise when not properly resolved. The strength of coherent coupling relative to the OKE depends critically on the sample position, with respect to the beam waist of the probe laser, as well as the angle subtended by the pump and probe beams. When the optics alignment is optimized for the OKE against coherent coupling the OHD-OKE signal is found to increase linearly with the local oscillator strength; the coherent coupling signal also appears to increase though the trend is not clear-cut.

PACS. 42.50.Md – Optical transient phenomena : quantum beats, photon echo, free-induction decay, dephasings and revivals, optical nutation, and self-induced transparency.

PACS. 78.47.+p – Time-resolved optical spectroscopies and other ultrafast optical measurements in condensed matter.

I. Introduction

The pump-probe optical Kerr effect (OKE) detected in the time domain with a resolution of tens of femtosecond (fs) is useful for the study of the coherent transients in liquids at room temperature [1-5]. Experimental procedure is more or less standardized. However, results are not always consistent because of experimental complexities, of which a few nontrivial ones will be mentioned in the next section. It is the ultimate objective of our endeavor to arrive at a textbook procedure so that the transient OKE experiment of liquid samples can be carried out routinely. Specifically, we have focused our attention on the so-called noises that are not easy to remove from the OKE data. This leads us to the identification of a physical process accompanying OKE, i.e. coherent coupling.

The coexistence of coherent coupling with OKE has already been discussed [1,5-7]. The pump and probe fields interact in the liquid sample to form a transient grating and, meanwhile, another pump field from the same pulse interacts with the grating leading to a third order polarization. The process runs in parallel with the OKE process. Due to the

ultrashort duration of the incident laser pulses the transient grating is conceivably more complicated than what one is accustomed to in frequency domain. Coherent coupling can overwhelm the Kerr signal when the pump and probe pulses overlap. Fine-tuning the optics alignment is useful for discriminating against coherent coupling as well as the stray signals. This, along with the ensuing results, will be given in the section on results and discussion.

II. Experimental

The very first step towards a successful OKE experiment, after the apparatus has been set up according to references [5] and [8], is the background noise suppression. The stray light polarized along the OKE-signal field, E_{OKE} (Fig. 1), has to be cleaned up. It arises mainly from three sources: Mie scattering, stray birefringence, and coherent coupling. Particles of proper size inside the sample cell walls and suspending in sample liquids can cause Mie scattering and hence stray light. Because of this a 1 mm light path cell (made by NSG Precision Cells, Inc.) specially selected for low light scattering is used; oftentimes some locations in the cell wall are found to have less light scattering than the other locations. A 1 mm sample-cell has advantage over the 10 mm cuvette in reducing liquid convection that will lead to dynamic Mie scattering if sample is not completely free of particles. The stray birefringence caused by the optics is coped with by using the cross-polarizer pair of the highest extinction ratio available (at least 10^{-6} with the Karl-Lambrecht product) and a X/4-wave plate. Note that mica wave plates are found to way surpass quartz ones in background suppression. After background noise has been suppressed to a tolerable level, we introduce the local oscillator field (E_{LO}, upper-left, Fig. 1) by tipping the X/4-wave plate either clockwise or counter-clockwise for $\sim 1°$ or less. The E_{LO} thus introduced interferes with the feeble optical Kerr field, E_{OKE}, leading to the greatly enhanced OHD-OKE signal.

Of no less importance are the spatial overlap in the sample cell of the pump and probe beams and the imaging of the coherent signal to the photo-detector as well. Fig. 1 shows the layout of the optics that we used for this purpose. The collimated pump and probe beams ($\sim$ 1 mm cross section) subtend an angle (β) of $\sim$ 9" as they are focused to

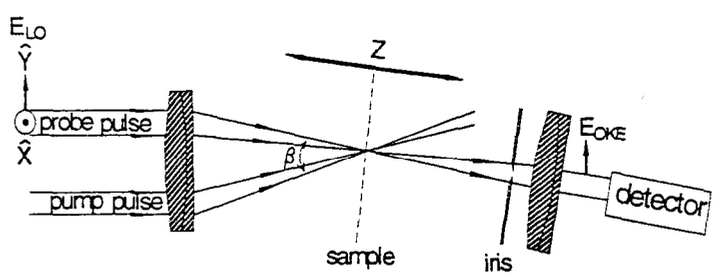

FIG. 1. **A** layout of the pump-probe optical Kerr experiment with ultrashort laser pulses. Only components of interest are shown. Probe field is polarized along $\hat{X}$ pointing out of the paper plane, shown by $\odot$ at upper left. Pump field polarization bisects, and hence has equal projection along, X and Y. Broken line indicates sample cell orientation.

the sample with a f/6 cm lens. Each beam subtends an angle of $\leq 1°$ upon converging to the sample. The sample cell is usually tilted an angle of $\sim$ 18". The pump and probe pulses are derived from single fs laser pulse. Although they are allowed to cross in $\sim$ 30 μm by the focusing optics, they last for only 30 fs, i.e. only 9 μm into the sample liquid. Thus the light-matter interaction volume is indeed very small, from which the E_{OKE} generated by the third order polarization proceeds to the photo-detector. It is important to assure that the spatial overlap of the pump and probe beams does not extend into the cell wall and is well defined (by using the TEM_{00} laser mode and the optical components that cause as less wave front distortion as possible).

It is not trivial to image the E_{OKE} with proper wave vector from the interaction volume to the photo-detector. The iris in Fig. 1, whose diameter is usually set at a few tenths of millimeter, determines the direction of the E_{OKE} wave vector to be detected. It is important to assure that only the tiny interaction volume is imaged to the photo-detector. A meticulous alignment of the optics downstream from the sample (including two irises not shown) is thus needed. Thereafter, we proceed to search for the sample positions along the Z-axis (Fig. 1), which give the best Kerr signal with the least noise. The sample cell filled with standard liquid sample (such as $CBrCl_3$) is then carefully displaced across the probe-beam-waist making sure that the alignment of the optics up- and down-stream remains unchanged. The displacement of the sample cell follows the Z-axis shown in Fig. 1. At each position of the cell the arrival time of the probe pulse maximum at the sample minus that of the pump pulse maximum (i.e. the delay time τ) is varied well over a full pulse-width to generate an OKE profile (Kerr signal versus delay time). We have found that a displacement of the cell as short as 50 nm sometimes has profound effect on the OKE profile around zero delay.

With liquid $CBrCl_3$ and the alignment of optics as described above we usually observe without much difficulty some signal around zero delay at some sample Z-positions, which clearly stands out from the background at negative delay. This signal usually appears as noises that are, indeed, coherent coupling as to be explained in next section. We then embark on the optimization of the optics for the OKE signal against the so-called noises by fine-tuning the P-angle. For that we conveniently change the pump beam from its parallel position with respect to the probe beam at an increment of 0.00305" at a time. Coherent coupling is usually easier to observe than OKE, and it is not easy to tilt the optics for the latter. However, we have found to-date patience and hard work always pay; the sample Z-position and the β-angle are usually fine-tuned alternately and sometimes simultaneously. Additionally, we find the iris positioned before the lens (Fig. 1) necessary for obtaining a nice OKE profile. Although it is easier to discriminate against coherent coupling with the iris, we can not rule out the effect of non-linear refraction as in the case of a Z-scan experiment [9].

The execution of nonlinear optical processes benefit greatly from an fs laser profile that is short in duration and thus high-powered. Ultrashort laser pulses tend to be broadened as they traverse optical elements and arrive at the sample. As some coherent transients of interest to us occur in much less than 100 fs, the critical pulse width [10], pulse broadening due to group velocity dispersion (GVD) has to be taken care of. For this purpose we find it convenient to take the ultrashort pulses out of the prism-pair side of the Kerr-lens mode-locked (KLM) titanium:sapphire (Ti:Sa) laser resonator [11]. Another prism pair is then

introduced in the spatially dispersed and collimated laser beam to compensate for the GVD downstream. In this manner, the laser pulses seen by the liquid samples can be adjusted from > 100 fs to ~ 25 fs or less [1]. Precaution is also taken to assure that the GVD's encountered by the pump and probe pulses are as close as possible, and that the pulses are transform-limited.

III. Results and discussion

Fig. 2 shows the variation of the OKE profile with the displacement of the sample cell with respect to the probe beam waist. The label Zmm in the top trace of this figure refers to the initial position of the sample cell. The delay time resolution used is about 10 fs per step. As explained below, the noisy signals around zero delay in the top profile and, particularly, the bottom ones in this figure are caused by coherent couplmg. They appear as noises because the resolution of the delay time used is not high enough. Thus, the second and third profiles from top of this figure have higher Kerr content, as they appear to be less noisy. A Z-displacement increment much less than those shown in this figure is also found to have profound effect on the noises.

The OKE profiles obtained with a low delay time resolution (~ 9 fs) while the β angle (Fig. 1) was being fine-tuned are shown in Fig. 3. As in Fig. 2 the noisy signals around

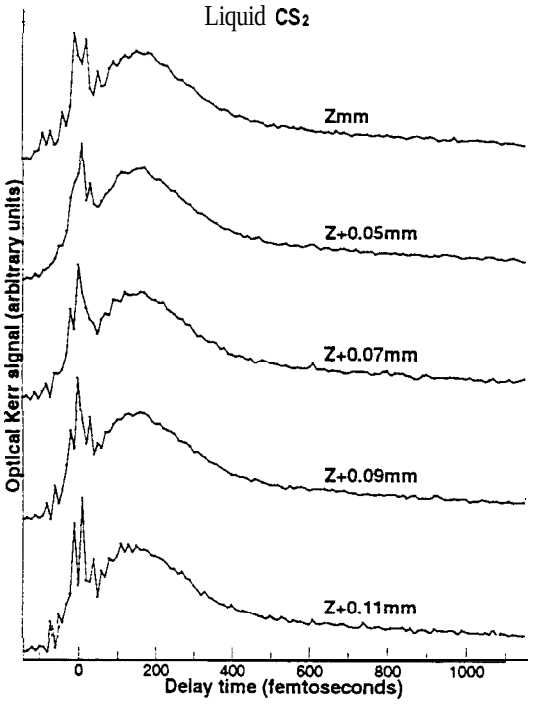

FIG. 2. Variation of the Kerr profile of liquid CS_2 with the displacement of the sample cell from the probe beam waist.

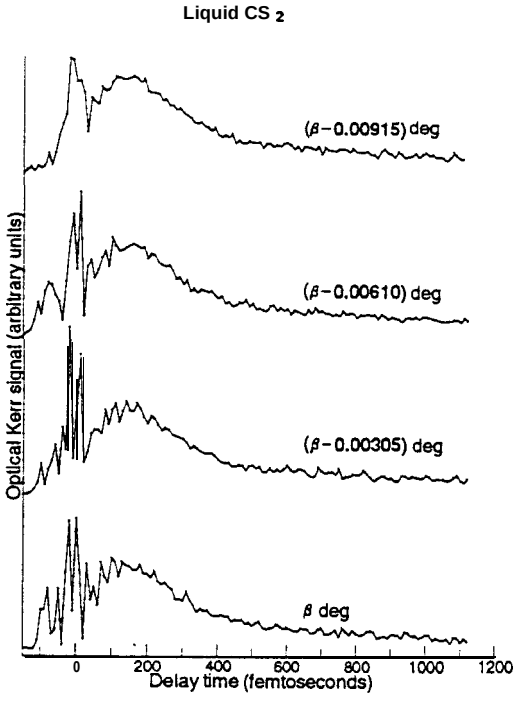

FIG. 3. Variation of the Kerr profile of liquid CS_2 with the angle subtended by the pump and probe beams β ❑ 9".

zero delay arise mostly from coherent coupling. Thus, the top profile has the highest Kerr content. Note that the order with which the noise pattern around zero delay changes with the β angle is not necessarily the same as shown in this figure. As shown in Fig. 2 and Fig. 3, the strength of coherent coupling relative to that of Kerr effect is very sensitive to a change in the β angle, which is set at $\sim 9^{\circ}$ to begin with, and in the sample Z-position.

After a persistent and most of the time tedious adjustment of the sample Z-position and the β angle a liquid CS_2 OKE profile similar to the top trace of Fig. 4 is obtained using the highest resolution available, 0.33 fs per step. Note the fast oscillation around zero delay and the stronger broad structure underneath. The former overwhelms the latter in the bottom profile when a different combination of Z-position and β angle is used. Their strength becomes comparable in the middle profile when still another combination is used. The fast oscillation around zero delay is attributed to coherent coupling and the broad structure underneath to the non-resonant electronic Kerr response that is instantaneous and hence can be represented with a delta function. The broad structure to the right arises from the delayed nuclear Kerr response that is causal (i.e. has memory). As expected they are free of coherent coupling. Note that the fast oscillations shown in this figure would have appeared as noises if the delay time resolution used were not high enough, which is usually the case. Similarly, if the laser pulses are not short enough for resolving the electronic response peak [1], coherent coupling (if not suppressed) will simply appear as noises in the leading portion of an OKE profile.

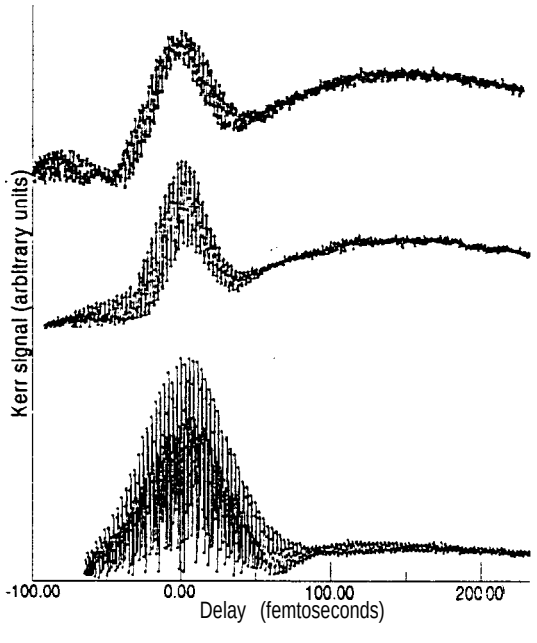

FIG. 4. Variation of the CS_2 Kerr profile with adjustments of the β angle and sample Z-position (Fig. 1) and other factors described in the text. Negative delays means earlier arrival of the probe pulse maximum at the sample relative to the pump pulse maximum.

The most convincing evidence for coherent coupling is the interference fringes (fast oscillations, Fig. 4) and their period (2.7 fs). The former is to be explained below; the latter agrees with the carrier wavelength (820 nm) of the mode-locked Ti:Sa laser used. A much weaker sequence of interference fringes with half the period of the major one is also observed in the bottom trace of Fig. 4. With the $CBrCl_3$ liquid a second sequence almost as strong as the fundamental one is also observed.

The variation of the OHD-OKE intensity as a function of the E_{LO} field strength is shown in Fig. 5. Dots in the figure refer to the maximum value of the prompt (delay 0) response as shown by the upper trace of Fig. 4. Crosses represent the electronic response, as they are obtained by subtracting the amplitude of the fast oscillation from the maximum value. Hollow triangles in Fig. 5 refer to the maximum value of the very broad structure to the right of the prompt response in Fig. 4. They correspond to the delayed nuclear response. Both the electronic response (x's) and the nuclear response (A's) increase linearly with the local oscillator field. As shown by the circle datum-points, the amplitude of the fast oscillation increases slowly with the local oscillator field though the trend is not clear-cut. Note that the optical alignment, with which the data were taken, is optimized for OKE against coherent coupling (the fast oscillation). We mention in passing that for the ultrashort laser pulses used the peak electronic Kerr response (x's, Fig. 5) of CS_2 is slightly weaker than the peak nuclear response (A's, Fig. 5). With broader laser pulses the electronic response will be much weaker than the nuclear response and hence show up as an asymrnetry in the broad nuclear response profile [1].

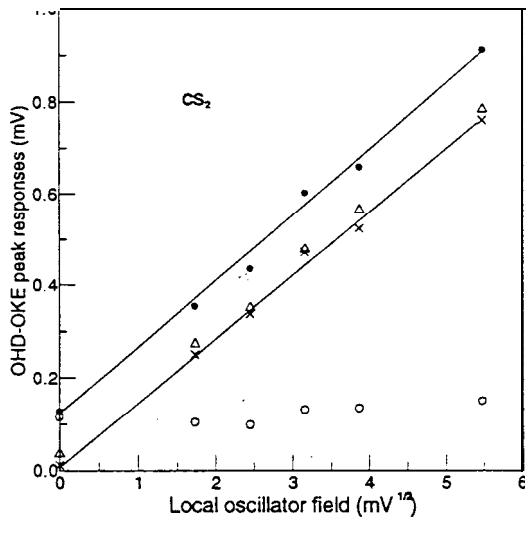

FIG. 5. The peak prompt (•) and nuclear (A) Kerr responses of liquid CS_2 as a function of the local oscillator strength. Crosses, peak prompt-response (•) minus the amplitude of the fast oscillation (o), stand for the electronic response. Optics alignment is optimized for OKE against coherent coupling.

Of the OKE data presented above two nonlinear optical processes are involved: the normal OKE (optimized) and the coherent coupling (greatly suppressed). We now proceed to describe the processes with the third order polarization given by Oudar [7], which pertains to the field polarization shown in Fig. 1,

$$P_Y^{NL}(t) = e^{i\omega t}\left\{\begin{array}{l} \frac{2}{3}\sigma\hat{E}_2(t)|\hat{E}_1(t)|^2 + \hat{E}_2(t)\int_{-\infty}^{\infty}\mathbf{b(t-t')}|\hat{E}_1(t')|^2dt' \\ +\hat{E}_1(t)\int_{-\infty}^{\infty}[\mathbf{a(t-t')} + \frac{1}{2}\mathbf{b}(t-t')]\hat{E}_2(t')\hat{E}_1^*(t')dt' \end{array}\right\}, \tag{1}$$

where subscript 1 refers to the pump pulse and 2 to the probe pulse. $\hat{E}(t)$ in equation (1) stands for the modulation envelope of the fs laser fields,

$$\vec{E}(\vec{r},t) = \frac{1}{2}\left[\hat{E}(t)e^{i(\vec{k}\cdot\vec{r}-\omega t)} + C.C.\right] \tag{2}$$

where w is the carrier frequency. The first term of equation (1) corresponds to the instantaneous electronic response (with the response function a), which is adiabatic as no electronic resonance is involved (liquid CS_2 does not absorb 820 nm). It is responsible for the broad structure underneath the fast oscillation around zero delay. The second term corresponds to the causal nuclear response, since the response function b has memory, i.e. is not a $\delta(t-t')$ function. It is responsible for the very broad structure to the right of the zero-delay structure. The nonlinear polarization $P_Y^{NL}(t)$ arising from the first two terms generates the normal OKE field $\vec{E}_{OKE}(t)$ that is in phase quadrature with the transmitted probe field $\vec{E}_2(t)$, X-polarized (Fig. 1). The last term gives rise to coherent coupling, from which we infer that at time t' the pump and probe fields split from single laser pulse interfere in the liquid sample, via the response function $a(t-t') + \frac{1}{2}\mathbf{b}(t-t')$, to form a transient grating [12]. At the detection time t another pump field $\vec{E}_1(t)$ from the same pulse interacts with the grating leading to $P_Y^{NL}(t)$ that produces an electric field $\vec{E}_{coh}(t)$ with appropriate wave vector [12-13].

Fig. 6 shows the phase matchings for OKE (top) and coherent coupling. Phase matching for OKE is automatically satisfied regardless of the angle (β) of overlap of the pump and probe beams [8,14], since the phase-matching factor $\mathrm{sinc}(\Delta kL/2)$, L being the light-matter interaction length, is vanishing, i.e. $\Delta\vec{k} = \vec{k}_2 - \vec{k}_1 \cdot 1 - \vec{k}_1 - \vec{k}_2 = 0$ [8]. Note that the signal field $\vec{E}_{OKE}(t)$ is generated collinear with the probe field, and that the pump pulse generates both the $\vec{k}_1$ and the conjugate $-\vec{k}_1$[8].

For coherent coupling the wave vector matching for the formation of the transient grating is expressed as

$$\vec{q} = \pm(\vec{k}_2 - \vec{k}_1), \tag{3}$$

where $q = 2k\sin\beta/2$ is the grating wave vector [12], k being the carrier wave length of the fs laser. The plus sign preceding the parentheses in equation (3) corresponds to positive $\vec{q}$ shown by the boldface arrow in the middle diagram (right half) of Fig. 6. Negative $\vec{q}$ is similarly defined. In keeping with this sign convention we have, for the first order diffraction of the second pump field off the transient grating [12-13],

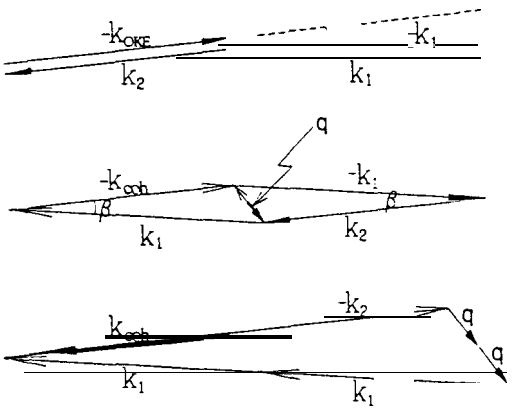

FIG. 6. Wave vector matching for OKE (top) and coherent coupling. **q** stands for the grating wave vector: the boldface arrow positive; the opposite arrow, negative.

$$\vec{q} = \pm(\vec{k}_{coh} - \vec{k}_1). \tag{4}$$

If the momentum imparted to the sample during grating formation exactly cancels that for the pump-field scattering ($\Delta\vec{q} = 0$), we take the difference of equations (3) and (4) to get $\vec{k}_{coh} = \vec{k}_2$. Thus, the coherent coupling signal that occurs in the first order diffraction propagates along with the OKE signal. The momentum conservation is shown in the middle diagram (left half) of Fig. 6. Taking the sum of both sides of equations (3) and (4) leads to

$$\vec{k}_{coh} = 2\vec{k}_1 - \vec{k}_2 \pm 2\vec{q}. \tag{5}$$

This coherent coupling process imparts a net momentum ($\hbar$ omitted) of $\Delta\vec{q} = 2\vec{q}$ to the transient grating. The corresponding signal field is collinear with the probe field, as shown in the bottom diagram of Fig. 6, just like the case of $\Delta\vec{q} = 0$. This makes it very difficult to optimize the OKE signal against the coherent coupling that occurs in the first order diffraction off the transient grating, as is actually observed. Note that we need not concern the $\Delta\vec{q} = -2\vec{q}$ scattering since the corresponding $\vec{k}_{coh} \neq \vec{k}_2$.

Difficult as it is to experimentally separate coherent coupling from OKE they are, after all, different in terms of the underlying mechanisms and the response functions. The response function for coherent coupling $\mathbf{a}(t - \mathbf{t}') + \frac{1}{2}\mathbf{b}(t - \mathbf{t}')$, equation (1), can not behave as fast as the delta function otherwise the phase of the two pump fields will cancel each other. It is thus causal just like $\mathbf{b}(t - \mathbf{t}')$ for OKE, the second term of equation (1). However, its response time should not be any slower than the pulse duration ($\leq$ 30 fs), otherwise the transient grating can not be built up so rapidly. Thus, material response due to the low-frequency phonon modes and the, relaxational modes, though active in the normal OKE, contributes little to coherent coupling (because slow in rising) [6]. Furthermore, the coherent coupling, including both $\Delta\vec{q} = 0$ and $\Delta\vec{q} = 2\vec{q}$, needs a transient grating to conserve momentum and hence depends on the scattering geometry whereas OKE does not at all. It is conceivable that by fine-tuning the β-angle and sample Z-position we shift the maximum of the first order diffraction away from the iris (Fig. 1) and thus weaken coherent coupling. Note that the iris is found crucial in the scattering geometry.

The OKE signal field, $\vec{E}_{OKE}(t)$, is inevitably feeble and is thus enhanced by OHD, i.e. by interfering with $\vec{E}_{LO}$ (Fig. 1), where $\vec{E}_{LO}(t) \propto ic\vec{E}_2(t)$ and $c^* = c \ll 1$ result from tipping the X/4 wave plate ≤ 1". Thus, the OHD-OKE signal can be expressed as

$$S_Y(t) \propto \mathrm{Re}\left[\vec{E}^*_{LO}(t)\vec{E}_{OKE}(t)\right] = \mathrm{Re}\left[\hat{E}^*_{LO}(t)\hat{E}_{OKE}(t)\right]. \tag{6}$$

Note that $\vec{E}_{OKE}(t)$ and $\vec{E}_{LO}(t)$ have identical phase and polarization ($\hat{Y}$), and hence their phases cancel each other in equation (6). Thus, no field-field interference fringes can be observed of the OHD-OKE signal. In view of equations (1) and (6) it appears reasonable to take the normal OHD-OKE (and normal OKE, $|\vec{E}_{OKE}(t)|^2$) as the intensity-intensity OKE in order to distinguish it from the coherent coupling process, which shall be termed the field-field OKE (vide infra). We believe it is inappropriate to consider this coherent coupling signal as artifacts as has been done in the related fields of research. Equation (6) also shows the linear dependence of the OHD-OKE signal on the local oscillator field, to which the data presented in Fig. 5 support.

The fact that the field-field interference fringes are observed as a function of delay (τ) around zero delay suggests that the phase of $\vec{E}_{coh}(t)$ has not been destroyed prior to signal detection. We then proceed to identify the field that interferes with $\vec{E}_{coh}(t) = i\hat{E}_Y(t)e^{i\omega t}$ [15], where $\hat{E}_Y(t)$ corresponds to the third term (in the braces) of equation (1). The polarization of the field we are looking for is set by the Y-polarization analyzer that we used. Taking the field in question as $\vec{E}^*_Y(t-\tau) = \hat{E}^*_Y(t-\tau)e^{-i\omega(t-\tau)}$ (vide infra) we have for the field-field OKE signal,

$$S_Y(\tau) \propto \mathrm{Re}\int_{-\infty}^{\infty} dt\vec{E}^*_Y(t-\tau)\xi\vec{E}_{coh}(t) = \mathrm{Re}\int_{-\infty}^{\infty} dt\,\hat{E}^*_Y(t-\tau)\xi\hat{E}_Y(t)e^{i\omega\tau}, \tag{7}$$

where ξ, reflects the scaling down of the coherent coupling field experimentally. Equation (7) shows that the field-field OKE signal oscillates rapidly according to $e^{i\omega\tau}$. This accounts for the stronger sequence of interference fringes mentioned above. The period of oscillation, 2.7 fs, that we observed agrees with the carrier frequency (w) of the fs laser used. We believe the $\vec{E}^*_Y(t-\tau)$ field that interferes with $\vec{E}_{coh}(t)$ is not the probe field [6]. Though the probe field is delayed by τ with respect to the pump field, it is polarized along X (see Fig. 1), i.e. perpendicular to $\vec{E}_{coh}(t)$. Note that equation (7) is basically identical to the ones given for the pump-probe transient absorption [16-17] and for the pump-probe OHD-OKE [5].

The best candidate for $\vec{E}^*_Y(t-\tau)$ is the local oscillator field. As shown by the circle datum-points of Fig. 5, the amplitude of the fast oscillation (the field-field OKE strength) appears to increase slightly with the local oscillator field, $E_{LO}(t-\tau)$, though the trend is not clear-cut. That the field-field OKE increases only slightly with local oscillator is understandable. The data presented in Fig. 5 pertain to the case of a greatly suppressed coherent coupling field and an optimized OKE field. This is because the fine tuning of the β angle and the sample Z-position has resulted in a scattering geometry, in which the first order maximum in the coherent coupling diffraction is shifted away from the iris of Fig. 1. ξ in equation (7) is thus much less than unit. Consequently, the slope of $S_Y(\tau = 0)$ versus $E_{LO}(\tau = 0)$ for coherent coupling, i.e. $\xi\vec{E}_{coh}$, is smaller than that for OKE, $\vec{E}_{OKE}(t)$.

Finally, we mention that poor contrast can result if the two interfering fields, i.e. $\vec{E}_{coh}(t)$ and $\vec{E}^*_Y(t-\tau)$, differ too much in amplitude. If this is true we can not exclude the contribution of poor contrast in the field-field interference to the broad structure underneath the fast oscillation in Fig. 4.

Taking $\vec{E}^*_Y(t-\tau)$ in equation (7) as the local oscillator field we can understand that the field-field OKE signal, if not suppressed $(\xi = 1)$, is not any weaker than the intensity-intensity OKE signal. In order for this to be true $\vec{E}_{coh}(t)$ in equation (7) needs be comparable with, or even stronger, than $\vec{E}_{OKE}(t)$ in equation (6). As prescribed by equation (1) this is not totally inconceivable. Coherent coupling efficiency is related to the scattering of the strong pump field off the transient grating. On the other hand, OKE effficiency is related to the interrogation of the after-effect of pumping using a weak probe.

IV. Conclusion

It is the main objective of this report to arrive at a textbook procedure so that the transient OHD-OKE experiment of liquid samples can be carried out routinely. Along this direction we have made significant headway. Using the highest delay-time resolution available we are able to illustrate several key details in the optics alignment, which help bring out the Kerr signal in respect to coherent coupling. The latter manifests itself in the interference fringes with a period consistent with the carrier wave of the ultrashort laser pulses used. The strength of the fringes is found to increase only slightly with the local oscillator field when coherent coupling is suppressed to bring out OKE.

The data presented in this report are accounted for with the existing theories on coherent coupling and OKE. The fringes observed along with the normal OKE signal are attributed to the interference between the local oscillator field and the nonlinear signal field. The latter arises from self-diffraction of the pump beam off the transient grating formed from the pump and probe fields. Shifting the diffraction maximum away from the iris of Fig. 1 can thus attenuate the amplitude of the fringes. This leads to an optimized OKE whose phase matching is automatically satisfied irrespective of the scattering geometry. This theoretical account to the interference fringes justifies the name, field-field OKE, for coherent coupling. As such we choose to call the normal OKE and OHD-OKE the intensity-intensity OKE.

Acknowledgments

Tzer-Hsiang Huang, Chia-Chen Hsu, and Tai-Huei Wei acknowledge financial assistance from National Science Council, Taiwan under contract Nos. NSC 87-2112-M-194-012, NSC 87-2112-M-194-007, and NSC 87-2112-M-194-013, respectively. They also acknowledge financial supports from the National Chung Cheng University for their individual proposals. Chao-Ming Fu acknowledges financial assistance from National Science Council, Taiwan under contract No NSC 86-2112-M-017-003.

References

† To whom all correspondences should be directed.

[1] Tzer-Hsiang Huang, *et al.*, IEEE J. Selected Topics in Quant. Electronics, 2, 756-768 (1996).
[2] M. Cho, *et al.*, J. Chem. Phys. 99, 2410-1428 (1993).
[3] Yong Joon Chang and Edward W. Castner, Jr., J. Chem. Phys. 99, 7289-7299 (1993).
[4] Toshiaki Hattori and Takayoshi Kobayashi, J. Chem. Phys. 94, 3332-3346 (1991).
[5] Dale McMorrow, William T. Lotshaw, and Geraldine A. Kenney-Wallace, IEEE J. Quantum Electron. QE-24, 443-454 (1988).
[6] S. Kinoshita, T. Ariyoshi, and Y. Kai, Chem. Phys. Lett. 257, 303-308 (1996).
[7] J.-L. Oudar, IEEE J. Quantum Electron. QE-19, 713-718 (1983).
[8] Gary L. Eesley, *Coherent Raman Spectroscopy,* (Pergamon, New York, 1981), chap. 3.
[9] Tai-Huei Wei and Tzer-Hsiang Huang, Opt. and Quant. Electronics, 28, 1495-1508 (1996).
[10] James G. Fujimoto, Generation *of high intensity femtosecond laser pulses and applications to studies of transient phenomena,* (Ph.D. thesis, Massachusetts Institute of Technology, 1984).
[11] Margaret M. Murnane, *et al., Mode-Locked Ti:Sapphire Laser: designs and guidelines for constructing a mode-locked titanium:sapphire* laser, Rev. 1.6, (Department of Physics, Washington State University, Pullman, Wa. 99164-2814, May 19, 1993).
[12] Hans Joachim Eichler, Peter Günter, and Dieter W. Pohl, *Laser-Induced Dynamic Gratings,* (Springer-Verlag, Berlin, 1986), Chap. 2.
[13] Arnnon Yariv, *Quantum Electronics,* 2nd ed. edition, (Wiley & Sons, New York, 1975) §14.9.
[14] Marc D. Levenson and Satoru S. Kano, *Introduction to Nonlinear Laser Spectroscopy, revised edition,* (Academic, San Diego, 1988), P. 20.
[15] Paul N. Butcher and David Cotter, *The elements of nonlinear optics,* (Cambridge University Press, Cambridge, 1990), Eq. (7.17).
[16] Z. Vardeny and J. Tauc, Opt. Comm. 39, 396-400 (1981).
[17] S. L. Palfrey and T. F. Heinz, J. Opt. Soc. Amer. B2, 674-679 (1985).